

Uniform and High Yield Carbon Nanotubes with Modulated Nitrogen Concentration for Promising Nanoscale Energetic Materials

Hao Liu^a, Yong Zhang^a, Ruying Li^a, Hakima Abou-Rachid^{b,*}, Louis-Simon Lussier^b and
Xueliang Sun^{a,*}

^a Department of Mechanical and Materials Engineering, University of Western Ontario, London, ON. N6A 5B9, Canada

^b Defence Research & Development Canada – Valcartier, 2459 Boulevard PieXI Nord, Quebec, QC. G3J 1X5, Canada

Abstract:

It is well known that pure polynitrogen systems are metastable. Recently, a theoretical study showed that when polymeric nitrogen chain is encapsulated in a carbon nanotube, it will be stable at ambient pressure and room temperature, which makes carbon nanotubes new promising as nanoscale energetic materials. Here, we report a systematic study of multi-walled carbon nanotubes with different nitrogen-doping amounts produced by aerosol assisted chemical vapor deposition, in which growth temperature, hydrogen flow rate and aerosol amount have been varied. The morphological and compositional changes of N-doped carbon nanotubes were characterized by means of scanning electron microscopy, transmission electron microscopy, and X-ray photoelectron spectroscopy. The detailed investigation of N-doped carbon nanotubes will provide a route to obtain evidence of the above theoretical prediction and will have potential applications in nanoscale energetic materials.

* Corresponding authors:

Xueliang Sun: E-mail address: xsun@eng.uwo.ca

Hakima Abou-Rachid: E-mail address: Hakima.Abou-Rachid@drdc-rddc.gc.ca

Introduction

Polynitrogen systems in which nitrogen atoms are connected with single bonds, have ultrahigh energies due to their significantly different bond energies from double and triple bonds of nitrogen, and have been proposed as a promising candidate to produce nanostructured energetic materials (Huheey et al. 1993). Polymeric nitrogen was theoretically predicted in 1992 (Mailhiot et al. 1992) and experimentally synthesized in 2004 (Eremets et al. 2004) but under high temperature and pressure as well as mechanical confinement, which is not desirable for practical applications of polymeric nitrogen used as an energetic material. So far, there have been no reports on synthesizing polymeric nitrogen that remains stable under ambient environment. On the other hand, carbon nanotubes (CNTs) have attracted great interest due to promising practical applications (Fennimore et al. 2003) resulting from their mechanical and electrical properties (Liu et al. 2008). While CNTs have been extensively studied, nitrogen doping has been considered a feasible strategy in a well-defined way for tuning physical and chemical properties of CNTs (Steohan et al. 1994). Recently, a theoretical study shows that when a polymeric nitrogen chain is encapsulated in a carbon nanotube, it will be stable at ambient pressure and room temperature (Abou-Rachid et al. 2008). Provided that the nitrogen doping within carbon nanotubes is realized in a controllable way, it will open a way to develop novel nanoenergetic materials, in which the combination between the polymeric nitrogen and CNTs is expected to be improved and the nitrogen doped CNTs may provide an alternative platform to realize composite nanoenergetic materials in a more viable

way. As a first step to experimentally synthesizing ambient environmental stable polynitrogen, the nitrogen-doped CNTs (CN_x) are synthesized initially. Among the methods for production of CN_x tubes, including arc-discharge (Cui et al. 2003), laser ablation (Nishide et al. 2003) and various techniques based on chemical vapor deposition (CVD) (He et al. 2005, Tao et al. 2007, and Maldonado et al 2006), aerosol assisted CVD (AACVD) appears to be the most suitable synthesis method for industrial scale production of CN_x tubes, in which stoichiometry control within the CN_x can be realized.

It should be noted that the successful incorporation of nitrogen atoms within the graphitic carbon cylinders strongly depends on the choice of precursor, catalyst, reaction temperature, reaction time, gas flow rate and pressure. Although some articles on the synthesis of CN_x tubes (He et al. 2005, Tao et al. 2007, and Maldonado et al 2006) have been published, the dependence of the quality of nanotubes on the involved experimental factors has not been well determined and it is difficult to compare them due to different experimental setups.

In this study, we describe the systematic study of the effects of various parameters on the growth of nitrogen-doped carbon nanotubes by AACVD, aiming to explore structural trends in CN_x tubes as a function of the synthesis parameters and thereby to open a new route to develop nanoenergetic materials with controllable nitrogen concentration.

Experimental procedure

The substrate used was a Si wafer with a 600 μm oxidation layer. Before the CN_x tube growth, the substrate was sputtered with a thin aluminum buffer layer of 30 nm thickness in order to obtain uniform and high density CN_x 错误!未定义书签。. The sputtering was carried out under the pressure of 4.0 mTorr and a power of 300 W.

The synthesis of CN_x tubes was carried out by a home-made AACVD system, initially developed for producing pristine CNTs (Zhang et al. 2009). It was basically composed of three different parts: an aerosol generator (Type 7901, RBI, France), a modified quartz chamber placed in a furnace (home made) and a gas trap for the exhausting gases. The method was based on the decomposition of an aerosol spray consisting of a liquid hydrocarbon source and an evaporable catalyst for the CNTs' formation. There were three argon inlets and one hydrogen inlet in this system. One inlet with carrier gases flowed through the aerosol solution and then carried aerosol into the reaction chamber. An additional argon inlet enables dilution of the obtained aerosol mixture. The Hydrogen was also introduced into the reaction chamber from its inlet. The metal catalyst precursor $\text{Fe}^{+3}(\text{acetylacetonate})_3$ was dissolved in acetonitrile (CH_3CN) which serves as a solvent for the aerosols and as a source of carbon and nitrogen. The concentration of Fe-ions in acetonitrile was 1.1 mM. The solution was placed inside a sonication generator and kept at constant room temperature during the synthesis at this temperature by cooling water.

The experiments were performed as follows. The pretreated silicon substrate was placed in a ceramic boat, inside the chamber. The furnace was heated to a temperature between 700°C and 1000°C after a 20-minute purge of air in the chamber by 400

standard cubic centimeters per minute (sccm) argon. As soon as the target temperature was reached, the aerosol droplets were produced by ultrasonication at a frequency of 850 KHz and transported by argon gas introduced from one inlet with a flow rate between 550 and 2500 sccm. At the same time, hydrogen was introduced with a flow rate between 200 and 2500 sccm as the reaction gas which reduced the catalyst precursor to form the active Fe^0 catalyst during the continuous injection. One additional argon inlet was employed to keep the total gas flow rate of 4000 sccm in the reaction chamber. In this experiment, the growth time was 30 minutes. At the end of the experiment, the aerosol generator and furnace were turned off. Gases kept passing through the reactor until the furnace cooled down to room temperature. The experiments were performed at atmospheric pressure. The samples were characterized by various analysis techniques including Hitachi S-4800 field-emission scanning electron microscope (SEM) operated at 5.0 kV, Philips CM10 transmission electron microscope (TEM) operated at 80 kV and Multilab 3000 XPS system manufactured by Thermo VG Scientific. The XPS data was collected with a dual anode x-ray source using Mg K irradiation with the energy of 1253.6 eV. Binding energies were measured using a hemispherical energy analyzer with fixed pass energy of 50 eV that gave an energy resolution of approximately 1.1 eV. The data was analyzed using an XPS data analysis software, Advantage, version 3.99 developed by Thermo VG Scientific. Fittings of the peaks were performed using Gaussian-Lorentzian product function and Shirley background algorithm. The sensitivity factors were also taken into account when we did the quantitative analysis.

Results and discussion

1. Effect of temperature

Temperature has a great effect on the morphology and structure of CN_x tubes. In our experiments, when the temperature was controlled ranging from 750 to 950°C, CN_x tubes were formed on the substrate and few tubes were observed when temperature was outside this temperature range. Fig. 1(a)-(c) display the scanning electron microscopy (SEM) images of the CN_x tubes synthesized at 750, 870 and 950°C revealing that the CN_x tubes grow perpendicularly to the substrate, forming flakes of ‘parallel’ aligned nanotubes. The length of the tubes produced at 750°C is less than 10 μm . As the temperature increased to 870°C, tube lengths up to 100 μm were observed. Further increase of the temperature to 950°C, however, reduced the length to 70 μm . Detailed discussion will be given later.

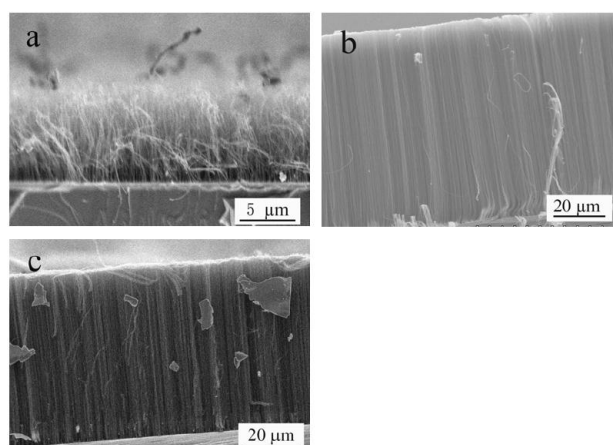


Figure 1 SEM images of CN_x tubes synthesized at 750°C, 870°C and 950°C

The structural change of the nanotubes as a function of the temperature is presented in Fig. 2 using representative transmission electron microscopy (TEM) images of CN_x tubes synthesized at different temperatures. The CN_x tubes produced at

all of these temperatures exhibit a bamboo-like structure with periodic compartments. The density of the compartments increased while the diameter of the tubes was kept almost unchanged as the temperature increases. The formation of CN_x tubes with bamboo-like structure is caused by the presence of nitrogen in the graphitic network, which induces curvature of the graphitic layer (Lee et al. 2003).

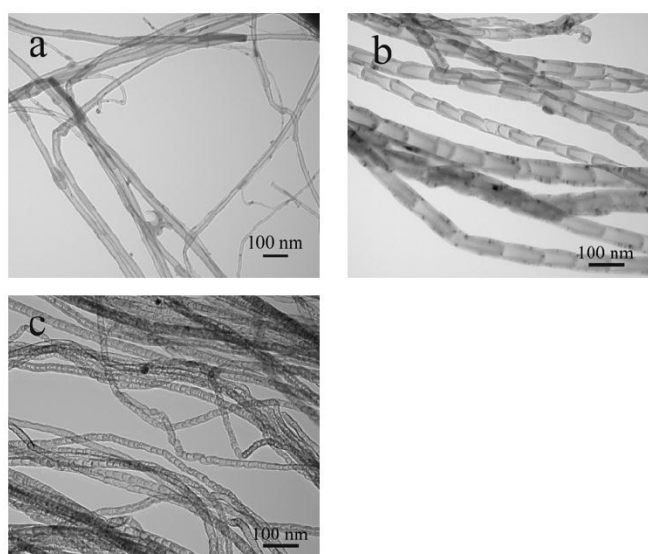


Figure 2 TEM images of CN_x tubes synthesized at 750°C, 870°C and 950°C

To determine the nitrogen concentration in the CN_x , X-ray photoelectron spectroscopy (XPS) analysis was carried out. Fig.3 displays XPS spectra taken from the CN_x synthesized at different temperatures. Fig. 3 shows the N 1s signals from these CN_x tubes synthesized at all temperatures. The asymmetric N 1s spectra indicate the existence of several components, which can be fitted into four peaks. The peaks around 399 eV, 401 eV, 403 eV and 405 eV correspond to pyridine-like nitrogen, graphite-like nitrogen, oxidized nitrogen and physisorbed nitrogen, respectively (Tao et al. 2007 and Liu et al. 2010). Pyridine-like nitrogen atoms contribute to the π system with a pair of pi electrons and only bonded to two C atoms ($C-N=C$). The

graphite-like nitrogen corresponds to highly coordinated N atoms substituting inner C atoms on the graphite layers.

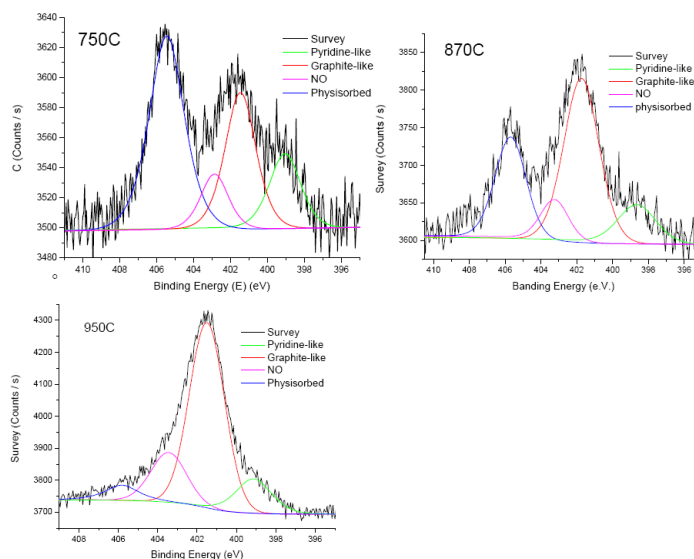


Figure 3 XPS plot of CN_x tubes synthesized at 750°C, 870°C and 950°C

To investigate the electronic structures of N atoms systematically, N1s XPS spectra are summarized in Table 1.

Table 1

Temperature	Nitrogen content	Pyridine-like	Graphite-like	NO	Physisorbed
750°C	1.7%	15.4%	28.1%	10.2%	46.3%
870°C	2.0%	10.0%	49.4%	11.4%	27.5%
950°C	4.0%	9.4%	61.9%	19.1%	9.6%

The N content contained in the nanotubes, defined as N/C at%, is estimated by the area ratio of the nitrogen and carbon peaks (Nath et al. 2000). As the temperature increases, the nitrogen content of the CN_x tubes increases from 1.7% to 4.0%. From

Table 1, it is also noteworthy that the ratio of graphite-like nitrogen increases significantly, while that of physisorbed nitrogen decreases greatly as the temperature increases. At higher temperatures, the pyrolysis of $C\equiv N$ in acetonitrile is enhanced compared with the case at low temperatures. Therefore more nitrogen atoms diffuse into the catalyst to contribute to the growth of CN_x tubes, and we observe an increase in nitrogen content at higher temperature. The increase in nitrogen content is also consistent with the increase in bamboo density from our TEM observation in which the bamboo density increases as the nitrogen contents increase. Since the graphite-like nitrogen has higher energy than the pyridine-like nitrogen (Chen et al., 2006 and Wang, 2006), nitrogen atoms prefer occupying the positions as graphite-like nitrogen rather than pyridine-like nitrogen for higher stability. It is expected that the graphite-like nitrogen is more favorable at higher temperatures/or increasing temperatures. As a result, the content of graphite nitrogen increases gradually from 28.1% to 61.9%. This observation agrees Van Dommele et al. (Van Dommele et al., 2008). Different references also report the relationship of nitrogen content and experimental temperature. The conclusion varies depending on different nitrogen precursors. Most of them concluded that the nitrogen content decreases or does not change as the temperature increases (He et al. 2005, Chen et al. 2006, Van Dommele et al. 2008, Tang et al. 2008, Choi et al. 2005, and Liu et al. 2005), but there is one reference reporting the same tendency as we observed (Yang et al. 2005). We find that when C-N or H-N bands containing precursors are used in experiments, the nitrogen content decreases with the temperature. However, when a $C\equiv N$ band containing the

precursor is employed, the nitrogen content has an opposite trend. The reason might be that the pre-existing C-N bond will be broken at high temperature to which the nitrogen content decrease is attributed. On the contrary, high temperature is beneficial for pre-existing C \equiv N bond to decompose into C-N bond which is considered to be the key factor to pursue CN_x tubes. We also observed that the length of the CN_x tubes decreases from 80 μ m to 60 μ m as the nitrogen contents increase from 2.0% to 4.0%. The presence of nitrogen slowed down the nanotube growth significantly which is quite similar to other references (Maldonado et al. 2006, and Koos et al. 2009). This phenomenon is reasonable according to the theoretical calculations that the nitrogen atoms prefer to be at the tube edge and could inhibit the growth of the nanotubes once the edges are nitrogen-saturated (Sumpter et al. 2007).

2. Hydrogen effect

Due to the deposition of non-crystalline carbon around the catalyst particles, the overall synthesis process can be hindered. Hydrogen gas source is proposed for etching off amorphous carbon produced during the synthesis process in order to minimize poisoning of the catalyst (Biris et al. 2008).

Typical SEM images of the CN_x tubes, shown in Fig. 4, display vertically aligned tubes grown on the substrate. Without hydrogen (not shown), no tubes could be observed on the substrate. When hydrogen flow of 200 sccm was introduced, CN_x tubes with the length of 20 μ m were produced, and the length of the tubes increased to 100 and 130 μ m as the hydrogen flow rate increased to 1100 and then 2500 sccm.

From our examination, hydrogen is critical for triggering and enhancing the growth of CN_x tubes.

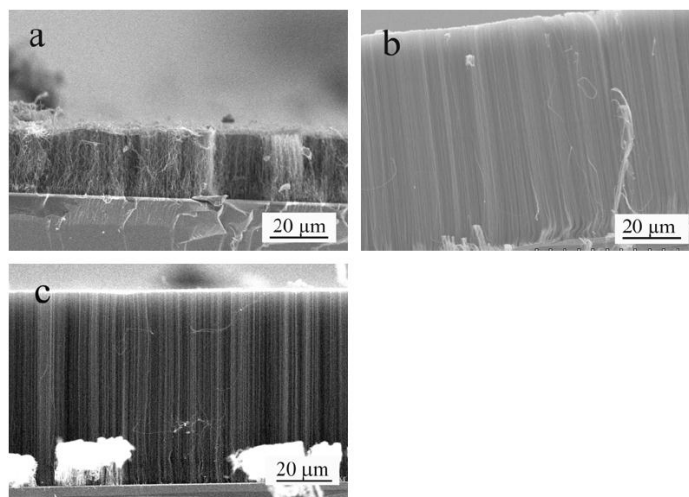


Figure 4 SEM images of CN_x tubes synthesized with 200, 1100 and 2500 sccm hydrogen

Fig. 5 shows typical TEM images of CN_x tubes synthesized at different hydrogen flow rates. All tubes demonstrate a bamboo-like structure. The compartment density changes scarcely as the hydrogen flow rate changes. The diameter of the tubes remains at around 40 nm regardless of the increase in hydrogen flow rate.

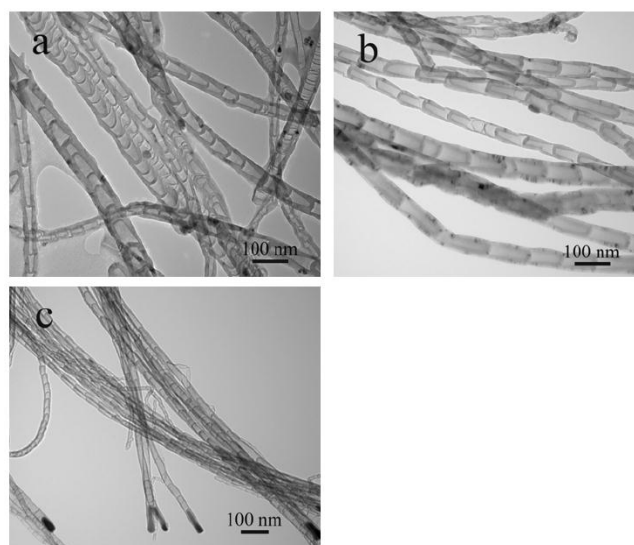


Figure 5 TEM images of CN_x tubes synthesized with 200, 1100 and 2500 sccm hydrogen

N 1s spectra of XPS and their summary are shown in Fig. 6 and Table 2,

respectively.

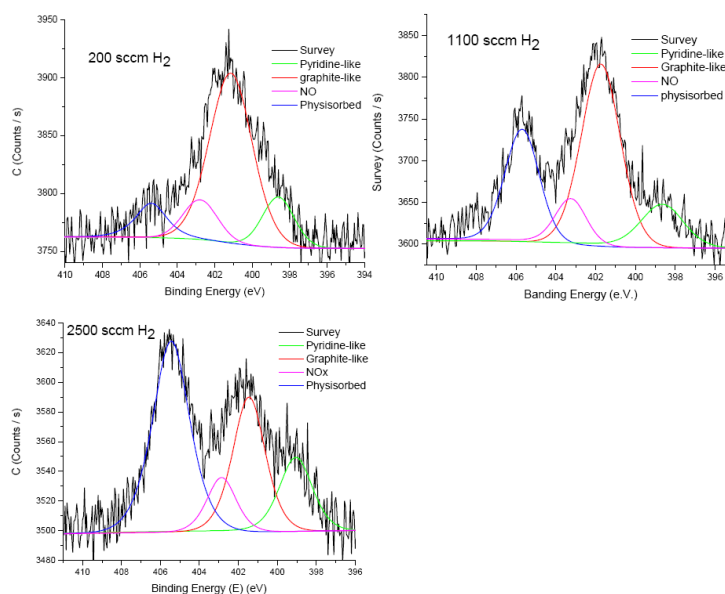


Figure 6 XPS plot of CN_x tubes synthesized with 200, 1100 and 2500 sccm hydrogen

With the increase of the hydrogen flow rate, nitrogen content within CN_x nanotubes increases at first but then decreases. However, as the hydrogen flow rate keeps on increasing although the nitrogen content difference is very small. Since hydrogen is critical for the growth of CN_x tubes, it is reasonable to observe a nitrogen content increase at the beginning of hydrogen flow rate increasing. After hydrogen exceeds the appropriate flow rate, the nitrogen content begins to decrease due to generation of HCN by the reaction $H_2 + CN^{\bullet} = HCN + H^{\bullet}$ at high temperature, as reported by Yan et al. (2003). Because HCN is more stable and less reactive than CH₃CN in gas phase, thus nitrogen is prohibited from doping into the tubes. This phenomenon is also observed by other authors (He et al. 2005 and Yan et al. 2003).

The XPS spectrum of each sample displays four sub-peaks as listed in Table 2.

Table 2

Hydrogen flow rate	Nitrogen content	Pyridine-like	Graphite-like	NO	Physisorbed
200 sccm	1.3%	11.9%	63.4%	12.1%	12.6%
1100 sccm	2.0%	10.0%	49.4%	11.4%	27.5%
2500 sccm	1.7%	15.4%	28.2%	10.1%	46.3%

The ratio of sub-peaks significantly changes as the hydrogen flow rate increases. The graphite-like nitrogen decreases and the physisorbed nitrogen increases with hydrogen flow rate, implying that hydrogen deters the incorporation of nitrogen into CN_x tubes (He et al. 2005). In this case, the nitrogen species in the nanotubes tends to change from graphite-like nitrogen to physisorbed nitrogen with the increase of hydrogen flow rate.

3. Aerosol spray effect

Aerosol spray offers the carbon and nitrogen source during the experiments. The flow rate of aerosol spray is viewed as another important parameter for the synthesis of CN_x tubes. SEM images in Fig. 7 show that the length of CN_x tubes was 40 μm at a small aerosol spray rate (550 sccm), and increased to 100 μm as the aerosol spray rate increased from 550 sccm to 1500 sccm.

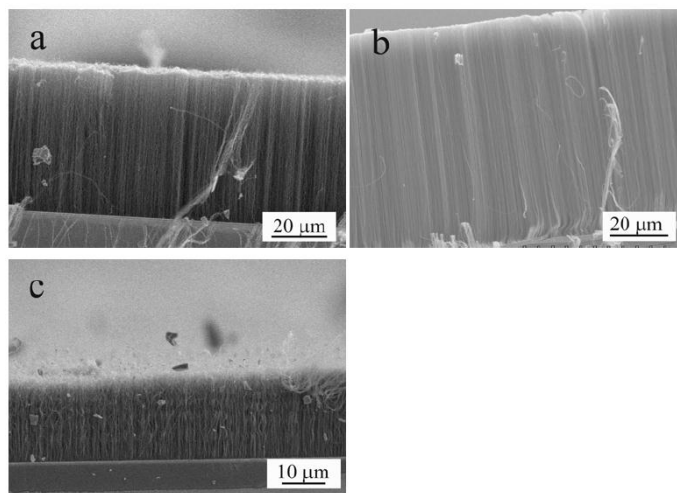


Figure 7 SEM images of CN_x tubes synthesized with 550, 1500 and 2500 sccm aerosol gas

As the aerosol spray rate went on increasing, the growth rate was hindered. When the aerosol spray rate reached 2500 sccm, the length of the CN_x tubes was only 20 μm. This phenomenon is reasonable. At a smaller aerosol spray rate (550 sccm), due to the shortage of carbon supply the growth of CN_x tube is limited while at a higher aerosol spray rate (2500 sccm), due to the overload of carbon supply's catalyst particles are covered with amorphous carbon which hinders the growth of CN_x tubes.

The TEM images in Fig. 8 indicate that all CN_x tubes, synthesized at 550 to 2500 sccm aerosol spray, exclusively exhibit a bamboo-like structure.

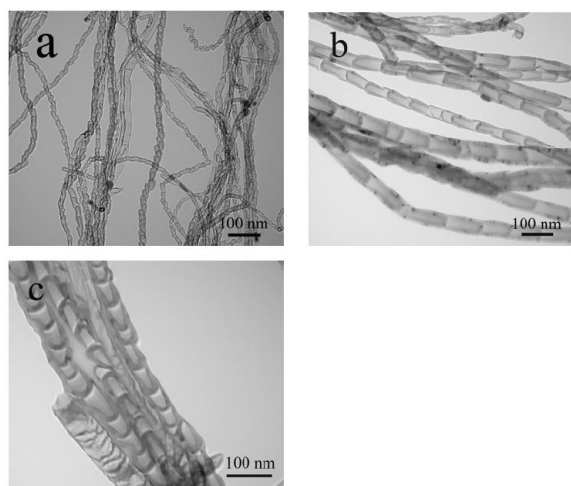


Figure 8 TEM images of CN_x tubes synthesized with 550, 1500 and 2500 sccm aerosol gas

Further, XPS spectra in Fig. 9 and the nitrogen composition distribution data in Table 3 show similar characteristics among the samples under different flow rates of aerosol spray.

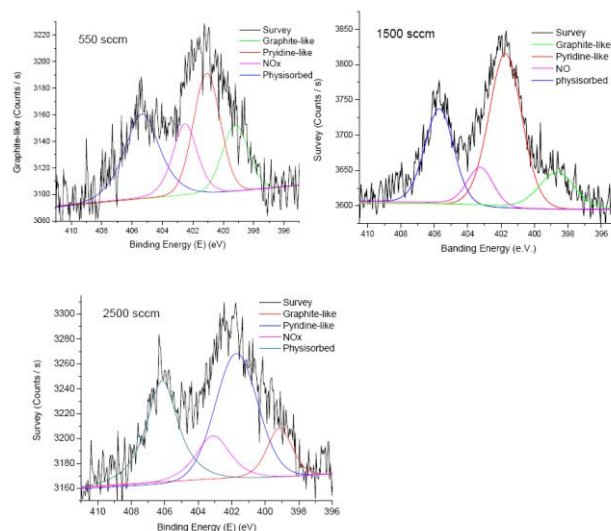


Figure 9 XPS plot of CN_x tubes synthesized with 550, 1500 and 2500 sccm aerosol gas

Table 3

Aerosol gas	Nitrogen content	Pyridine-like	Graphite-like	NO	Physisorbed
550 sccm	1.7%	17.6%	33.2%	18.1%	31.0%
1500 sccm	2.0%	10.0%	49.4%	11.4%	27.5%
2500 sccm	1.9%	10.7%	47.4%	13.9%	28.1%

Our observation is contradictory to other reports that nitrogen content increases as the nitrogen source increases in a certain range (Maldonado et al. 2006, Bulusheva et al. 2008, and Jang et al. 2004) but we noticed that both the nitrogen source and the carbon source are simultaneously employed in the reaction. During their experiments, the nitrogen source increased while carbon source was kept unchanged or even decreased. Actually, the nitrogen/carbon ratio changed with the increase in nitrogen source. Acetonitrile was used as both nitrogen and carbon source in our experiments,

which was different from the other experiments. Therefore, the nitrogen/carbon ratio was unchanged as the aerosol spray rate in our experiments increased. We can conclude that an appropriate aerosol spray rate is critical for the growth of CN_x tubes and nitrogen content is related to the nitrogen/carbon ratio instead of the aerosol spray rate.

Conclusion

In conclusion, the effects of important experimental parameters including temperature, hydrogen and aerosol spray on the growth of CN_x tubes have been studied by changing one parameter at a time. Our observations show that nitrogen content increases as the temperature increase and nitrogen tends to exist in the form of graphite-like structure which is more stable at higher growth temperature. Hydrogen is necessary for the growth of CN_x tubes. No tubes are observed without hydrogen and the growth rate of CN_x tubes increases with the hydrogen flow rate. However, excessive hydrogen deters the incorporation of nitrogen into the nanotubes and favors the formation of physisorbed nitrogen. Aerosol spray rate is crucial for the optimized growth rate of CN_x tubes, but brings little influence on the nitrogen doping and distribution in the nanotubes. Based on the results previously listed, it is possible to obtain nitrogen-doped carbon nanotubes with controlled concentration and structure by AACVD method, which will benefit the development of novel nanoenergetic materials.

Acknowledgements

Authors thank Dr. Sylvain Désilets for his fruitful discussions and Eng. Robert Stowe for his useful reading of this paper. This research was supported by Department of National Defence (DND), Natural Sciences and Engineering Research Council of Canada (NSERC), Canada Research Chair (CRC) Program, Canada Foundation for Innovation (CFI), Ontario Research Fund (ORF) Ontario Early Researcher Award (ERA) and the University of Western Ontario.

References

- Abou-Rachid, H., Hu, A., Timoshevskii, V., Song, Y. and Lussier, L.-S., (2008) A Polymeric Nitrogen Chain N_8 Confined inside a Carbon Nanotube, *Phys. Rev. Lett.*, 100, pp. 196401.
- Biris, A.R., Li, Z., Dervishi, E., Lupu, D., Xu, Y., Saini, V., Watanabe, F. and Biris, A.S., (2008) Effect of Hydrogen on the Growth and Morphology of Single Walled Nanotubes Synthesized on a Fe-Mo/Mg Catalytic System, *Phys. Lett. A.*, 372, pp. 3501-3507.
- Bulusheva, L.G., Okotrub, A. V., Kinloch, I. A., Asanov, I.P., Kurennya, A. G., Kudashov, A. G., Chen, X. and Song, H., (2008) Effect of Nitrogen Doping on Raman Spectra of Multi-walled Carbon Nanotubes, *Phys. Stat. Sol. (b)*, 245(10), pp. 1971-1974.
- Chen, H., Yang, Y., Hu, Z., Huo, K., Ma, Y. And Chen, Y., (2006) Synergism of C_5N Six-Membered Ring and Vapor-Liquid-Solid Growth of CN_x Nanotubes with Pyridine Precursor, *J. Phys. Chem. B.* 110(3), pp.16422-16427.
- Choi, H. C., Park, J. and Kim, B., (2005) Distribution and Structure of N Atoms in Multiwalled Carbon Nanotubes Using Variable-Energy X-Ray Photoelectron Spectroscopy, *J. Phys. Chem. B.* 109, pp. 4333-4340.
- Cui, S., Scharff, P., Siegmund, C., Spiess, L., Romanus, H., Schawohl, J., Risch, K., Schneider, D. and Klotzer, S., (2003) Preparation of Multiwalled Carbon Nantubes by DC Arc Discharge under a Nitrogen Atmosphere, *Carbon*, 41(8), pp. 1648-1651.
- Eremets, M. I., Gavriiliuk, A. G., Trojan, I. A., Dzivenko, D. A. and Boehler, R., (2004) Single-Bonded Cubic Form of Nitrogen, *Nature Materials*, 3, pp. 558-563.

Fennimore, A. M., Yúzvinsky, T. D., Han, W., Fuhrer, M. S., Cumings, J. and Zettl, A., (2003) Rotational Actuators Based on Carbon Nanotubes, *Nature*, 424, pp. 408-410.

He, M., Zhou, S., Zhang, J., Liu, Z. and Robinson, C., (2005) CVD Growth of N-doped Carbon Nanotubes on Silicon Substrates and Its Mechanism, *J. Phys. Chem. B*, 109(19), pp. 9275-9279.

Huheey, J. E., Keiter, E. A. and Keiter, R. L., (1993) *Inorganic Chemistry*, 4th ed.; New York: Harper-Collins, p. A31.

Jang, J. W., Lee, C. E., Lyu, S. C, Lee, T. J. and Lee, C. J., (2004) Structural Study of Nitrogen-Doping Effects in Bamboo-Shaped Multiwalled Carbon Nanotubes, *Appl. Phys. Lett.*, 84(15), pp. 2877-2879.

Koos, A. A., Dowling, M., Jurkschat, K., Crossley, A. and Grobert, N., (2009) Effect of the Experimental Parameters on the Structure of Nitrogen-Doped Carbon Nanotubes Produced by Aerosol Chemical Vapour Deposition, *Carbon*, 47(1), pp. 30-37.

Lee, Y. T., Kim, N. S., Bae, S. Y., Park, J., Yu, S. C., Ryu, H. and Lee, H. J., (2003) Growth of Vertically Aligned Nitrogen-Doped Carbon Nanotubes: Control of the Nitrogen Content over the Temperature Range 900-1100 °C, *J. Phys. Chem. B*, 107, pp. 12958-12963.

Liu, H., Zhang, Y., Arato, D., Li, R., Mérel, P. and Sun, X., (2008) Aligned Multi-walled Carbon Nanotubes Synthesized by Floating Catalyst CVD: Effects of Buffer Layer and Substrates, *Surf. & Coatings Tech.*, 202, pp. 4114-4120.

Liu, H., Zhang, Y., Li, R., Sun, X., Desilets, S. and Abou-Rachid, H., (2010) Structural and Morphological Control, Nitrogen Incorporation and Stability of Aligned Nitrogen-doped Carbon Nanotubes, *Carbon*, 48, 1498-1507.

Liu, J., Webster, S. and Carroll, D. L., (2005) Temperature and Flow Rate of NH₃ Effects on Nitrogen Content and Doping Environments of Carbon Nanotubes Grown by Injection CVD Method, *J. Phys. Chem. B*, 109, pp. 15769-15774.

Mailhiot, C., Yang, L. H. and McMahan, A. K., (1992) Polymeric Nitrogen, *Phys. Rev. B*, 46, pp. 14419-14435

Maldonado, S., Morin, S. and Stevenson, K.J., (2006) Structure, Composition, and Chemical Reactivity of Carbon Nanotubes by Selective Nitrogen Doping, *Carbon*, 44(8), pp. 1429-1437.

Nath, M., Satishikumar, B. C., Gobindaraj, A., Vinod, C. P. and Rao, C. N. R., (2002) Production

of Bundles of Aligned Carbon and Carbon-Nitrogen Nanotubes by the Pyrolysis of Precursors on Silica-Supported Iron and Cobalt Catalysts, *Chem. Phys. Lett.*, 322(5), PP. 333-340.

Nishide, D., Kataura, H., Suzuki, S., Trukagoshi, K., Aoyagi, Y. and Achiba, Y., (2003) High-yield Production of Single-wall Carbon Nanotubes in Nitrogen Gas, *Chem. Phys. Lett.*, 372(1-2), pp. 45-50.

Stoehan, O., Ajayan, P. M., Colliex, C., Redlich, Ph., Lambert, J. M., Bermier, P. and Lefin, P., (1994) Doping Graphitic and Carbon Nanotube Structures with Boron and Nitrogen, *Science*, 266, pp. 1683-1685.

Sumpter, B. G., Meunier, V., Romo-Herrera, J. M., Cruz-Silva, E., Cullen, D. A., Terrones, H., Smith, D. J. and Terrones, M., (2007) Nitrogen-Mediated Carbon Nanotube Growth: Diameter Reduction, Metallicity, Bundle Dispersability, and Bamboo-like Structure Formation, *ACS Nano*, 1(4), pp. 369-375.

Tang, C., Bando, Y., Golberg, D. and Xu, F., (2008) Structure and Nitrogen Incorporation of Carbon Nanotubes Synthesized by Catalytic Pyrolysis of Dimethylformamide, *Carbon*, 42(12-13), pp. 2625-2633.

Tao, X. Y., Zhang, X. B., Sun, F. Y., Cheng, J.P., Liu, F. and Luo, Z. Q., (2007) Large-Scale CVD Synthesis of Nitrogen-Doped Multi-Walled Carbon Nanotubes with Controllable Nitrogen Content on a $\text{Co}_x\text{Mg}_{1-x}\text{MoO}_4$ Catalyst, *Diamond Relat. Mater.*, 16(3), pp. 425-430.

Van Dommele, S., Romero-Izquierdo, A., Brydson, R., de Jong, K. P. and Bitter, J. H., (2008) Tuning Nitrogen Functionalities in Catalytically Grown Nitrogen-Containing Carbon Nanotubes, *Carbon*, 46, pp. 138-148.

Wang, E. G., (2006) Nitrogen-Induced Carbon Nanobells and Their Properties, *J. Mater. Res.*, 21(11), pp. 2767-2773.

Yan, H., Li, Q., Zhang, J. and Liu, Z., (2003) The Effect of Hydrogen on the Formation of Nitrogen-Doped Carbon Nanotubes via Catalytic Pyrolysis of Acetonitrile, *Chem. Phys. Lett.*, 380, PP. 347-351.

Yang, Z., Xia, Y. and Mokaya, R., (2005) Aligned N-doped Carbon Nanotube Bundles Prepared via CVD Using Zeolite Substrates, *Chem. Mater.*, 17, pp. 4502-4508

Zhang, Y., Li, R., Liu, H., Abou-Rachid, H., Lussier, L. and Sun, X., (2009) Aerosol-Assisted

CVD Synthesis of Aligned Carbon Nanotubes on Various Metal Substrates: Effects of Water, *Appl. Surf. Sci.*, 255, pp. 5003-5008